Journal of Nuclear Materials 400 (2010) 245–250

Contents lists available at ScienceDirect

Journal of Nuclear Materials

journal homepage: www.elsevier.com/locate/jnucmat

C and D reemission from mixed W–C–D layers during single-species and simultaneous irradiations of W with C^+ and D^+

I.A. Bizyukov [a], J.W. Davis [a], A.A. Haasz [a,*], P. Brodersen [b]

[a] University of Toronto Institute for Aerospace Studies (UTIAS), 4925 Dufferin Street, Toronto, Ontario, Canada M3H 5T6
[b] University of Toronto, Department of Chemical Engineering and Applied Chemistry, Toronto, Ontario, Canada

ARTICLE INFO

Article history:
Received 27 November 2009
Accepted 16 March 2010

ABSTRACT

We present new experimental results on the reemission of C and D from tungsten during single-species and simultaneous irradiations with 6 keV C^+ and 1 keV D^+ ion beams. The relatively low C fraction in the combined total beam flux (~4.5% $C^+/[C^+ + D^+]$) was selected to prevent the formation of a carbon overlayer during C^+ irradiation. The results show that the temperature dependence of D reemission from a mixed W–C–D surface is similar to that from pure W. In the case of a mixed W–C surface, the reemission of C was much lower than observed for pure carbon. Post-irradiation XPS analysis of the chemical bonding states of a W specimen irradiated at 973 K with 6 keV C^+ shows that carbon in the mixed W–C surface is primarily in the form of WC.

1. Introduction

The materials selected for ITER comprise beryllium on the first wall, graphite (or carbon-fibre composites) for the high-heat flux target plates in the divertor, and tungsten-coated surfaces in the baffle region of the divertor [1–3]. Plasma-facing materials will experience erosion due to plasma impact, leading to the release of impurities into the plasma. Some of these impurities (primarily Be, C, W and O) will in turn redeposit on plasma-facing surfaces, forming mixed-materials. The close proximity of carbon and tungsten in the divertor will likely lead to the formation of mixed W–C layers [4,5].

An earlier erosion experiment with a mixed W–C–D surface was performed with the use of a single ion beam of CH_3 radicals [6], prompting the current interest in this topic. More recent investigations of mixed W–C–D materials have employed dual ion beams to study processes such as kinematic sputtering [7,8], chemical erosion of C from a mixed surface [9,10], and the retention of deuterium in such mixed layers [11]. Most of these previous experiments followed well-established procedures used for studying single-element materials, with the objective to identify how mixed materials differ from their pure-element counterparts under ion irradiation. For example, pure W does not exhibit any chemical erosion under D^+ irradiation while pure-C materials (e.g., graphite and carbon-fibre composites) exhibit a prominent maximum in the temperature dependence curve of chemical erosion at around 700 K, e.g., [12]. In contrast, methane produced by chemical erosion from a mixed W–C–D surface exhibits a weak maximum at ~300 K and virtually disappears at higher surface temperatures [9,10]. Since mixed materials will inevitably be present in tokamaks with plasma-facing components made of different elements, it is important to investigate the behaviour of such materials under ion irradiation. Even if simple extrapolation from the characteristics of pure elements were to be attempted, confirmation with the expected material mix is warranted.

Irradiation of pure carbon with energetic (>100 eV) particles – both hydrogenic and non-hydrogenic – leads to the release of sub-eV C atoms at temperatures above 1000 K via radiation-enhanced sublimation, RES [13,14]. Irradiation of pure tungsten and pure carbon with D^+ also leads to the reemission of D atoms and D_2 molecules, and their respective intensities is a function of temperature [15]. Will such reemissions also occur from mixed W–C–D surfaces, and if they do, will they differ from those seen with the pure elements?

The objective of the present study is to measure the (i) reemission of deuterium (both atomic D and molecular D_2) from mixed W–C–D layers during simultaneous irradiation of tungsten by C^+ and D^+ ions, and (ii) reemission of C from mixed W–C layers at elevated temperatures using line-of-sight (LOS) mass spectroscopy. The mass spectrum of particles emitted from the surface will influence particle transport in the edge plasma, which may have an effect on the high recycling divertor concept currently under consideration for ITER.

2. Experiment

2.1. Experimental setup

Tungsten specimens were irradiated with independently controlled and mass–analyzed beams of C^+ and D_3^+ using the

* Corresponding author. Tel.: +1 416 667 7734; fax: +1 416 667 7799.
E-mail address: tonyhaasz@utias.utoronto.ca (A.A. Haasz).

0022-3115/$ - see front matter © 2010 Elsevier B.V. All rights reserved.
doi:10.1016/j.jnucmat.2010.03.010

dual-beam ion accelerator at the University of Toronto Institute for Aerospace Studies [16]. The C^+ and D^+ beam diameters were ~4 mm and ~5 mm, respectively, with the two beams overlapping in the central 4 mm diameter region. The beam intensities were adjusted to obtain the desired species ratio with sufficiently high ion fluxes to produce measurable signals. The C^+ energy was fixed at 6 keV while the D_3^+ energy was fixed at 3 keV to produce 1 keV/D^+. (Here we denote the incident particles as D^+ even though not all atoms in the molecular D_3^+ ion are charged.) The ion energies correspond to a mean projectile range of 11 nm for C^+ in W and 16 nm for D^+ in W [17]. The angle of incidence for each ion beam was 21° from the surface normal, forming a 42° angle between the two beams, and the target was normally biased to +30 V to suppress secondary electrons.

The ion beam fluxes were fixed at 0.5×10^{18} C^+ m^{-2} s^{-1} and 10.5×10^{18} D^+ m^{-2} s^{-1}. For the experiments where both beams were on, the C^+ fraction in the total incident ion flux was maintained at about 4.5%. However, variations in the C^+ and D^+ fluxes across the beam spots led to an uncertainty of about a factor of two in the C^+/D^+ flux ratio. Based on TRIDYN [18] computer simulations, the 4.5% C^+ fraction should be sufficiently low to maintain a steady-state mixed W–C–D surface (i.e., the number of implanted C atoms equals the number of reflected and sputtered C atoms) during simultaneous irradiations. Otherwise, the formation of a carbon overlayer (actually a mixed C–D layer) would tend to protect the W surface from interacting with the incident ions.

The W specimens were cut from a hot-rolled 25 μm thick W foil (99.96 wt.% pure) purchased from Rembar Company Inc. The frontal dimensions were 1×4 cm^2. Prior to irradiation, the specimens were cleaned with alcohol and baked in vacuum at temperatures of up to 1073 K. During irradiation, the specimens were resistively heated and their temperature was monitored with a K-type (chromel–alumel) thermocouple. The measurement accuracy was ~5 K at room temperature (RT), but we suspect that the specimen temperature was underestimated by up to 30 K at 900 K, due to the thermocouple being located a few mm away from the central part of the specimen. We have not corrected for errors in the thermocouple readings.

To compare the high-temperature C reemission (RES) from a mixed W–C layer, some experiments were also performed with pure carbon (pyrolytic graphite). While a thermocouple was used for measuring the temperature of W specimens, in the case of graphite a pyrometer was employed.

2.2. LOS-QMS detection

Particles emitted from the specimens during irradiation were directly detected by a line-of-sight quadrupole mass spectrometer (LOS-QMS) positioned about 60 mm away from the specimen, at an angle of 45° with respect to both the specimen normal and the plane containing the two beam lines. The typical pressure in the vacuum chamber during the experiment was $<2 \times 10^{-5}$ Pa, with corresponding mean free paths of >100 m for particles emitted from the surface. Therefore, emitted particles reach the detector of the QMS without collisions. The flux of emitted atoms and molecules was chopped with a 50 Hz tuning-fork type chopper before entering the QMS ionizer. A phase-sensitive detection system was used to separate the LOS signals from the background.

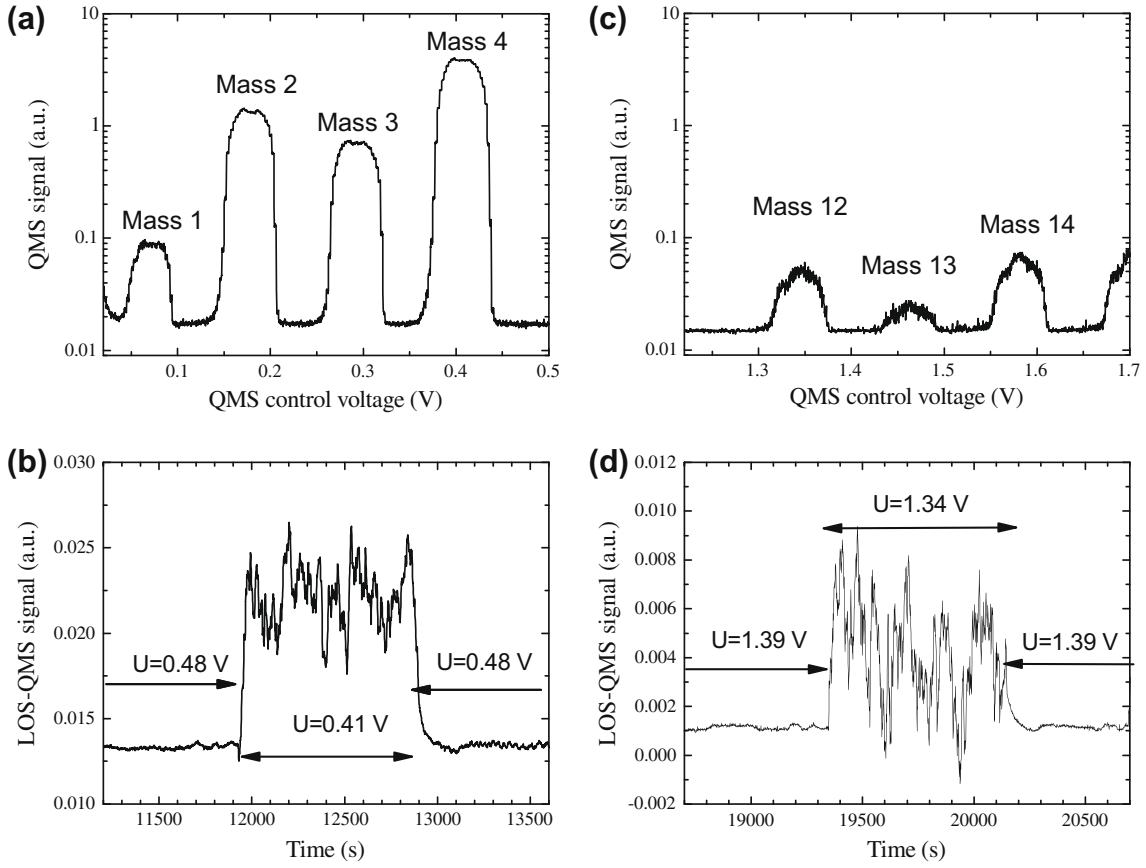

Fig. 1. LOS-QMS measurement of the reemitted D_2 and C particle flux. In (a) and (b) both C^+ and D^+ beams are always on; in (c) and (d) the C^+ beam is always on. The specimen surface was at RT. (a) *Low-range* mass spectrum obtained by QMS in the residual gas; (b) LOS background signal obtained at QMS control voltage $U = 0.48$ V; and D_2 reemission signal obtained at $U = 0.41$ V. (c) *Medium range* mass spectrum obtained by QMS in the residual gas; (d) LOS background signal obtained at $U = 1.39$ V; and C reemission signal obtained at $U = 1.34$ V.

The method of LOS-QMS signal analysis used here is demonstrated in Fig. 1 where the measurement of the mass 4 intensity is used as an example. Fig. 1a shows a typical 'low-range mass spectrum' of the *residual gas* for masses 1–4 during the bombardment of the W surface with D^+ and C^+ ions. We note that some high-energy (order of several 100's eV) beam particles reflected from the specimen will pass through the quadruple and will generate a background signal; this is shown in Fig. 1b for times less than 11,940 s. The relevant background for LOS-QMS detection is measured by setting the QMS control voltage U at a value where no signal is detected in the *residual gas* in Fig. 1a; in this example $U = 0.48$ V. Then, the control voltage is set to the value of $U = 0.41$ V, which corresponds to mass 4 at the mass-spectrum shown in Fig. 1a. At this setting the LOS-QMS system starts to detect D_2 molecules reemitted from the surface, as shown in Fig. 1b during the time span from 11,940 to 12,860 s. We note that the noise in the D_2 signal is much higher than that of the background. After 12,860 s the background signal was measured again and was found to be similar to the initial level. The difference between the level corresponding to mass 4 and the background level is assumed to be proportional to the intensity of the reemitted D_2 flux leaving the surface. Similarly, Fig. 1c shows the 'medium-range mass spectrum' in the *residual gas* and Fig. 1d shows the QMS-LOS signals corresponding to the reemitted C at elevated temperatures due to RES and the corresponding background.

2.3. XPS analysis

All X-ray photo-electron spectroscopy (XPS) measurements were obtained with a ThermoScientific K-Alpha X-ray Photo-electron Spectrometer, with monochromated Al K-alpha X-rays. The analysis spot was ~300 μm. Depth profiles were obtained by sputtering with a 2 keV Ar^+ ion beam; the depth scale has been calculated based upon fixed values for the sputter yield, independent of the surface concentrations. Surface elemental compositions were calculated from background-subtracted peak areas derived from transmission function corrected regional spectra. Sensitivity factors (Scofield) used to calculate the relative atomic percentages were provided by the manufacturer. The energy scale of the instrument was calibrated to metallic Cu2p, Ag3d, and Au4f features.

The errors associated with XPS quantification are derived from several sources, including uncertainty in the background function chosen to model the actual background structure, choices of integration boundaries, accuracy of the sensitivity factors, homogeneity/heterogenity of the species of interest within the sampling volume, etc. Factors such as signal-to-noise and peak intensity also play an important role. In general, the accuracy of the current measurements should be ±5–10%. We note that since the implantation depth of 2 keV Ar^+ ions in tungsten is ~2–3 nm, the ion-induced mixing zone should be limited to 2–3 nm, which is approximately equal to the depth resolution of XPS.

With regards to the accuracy of the bonding information, the percentage contributions are derived from mathematical modelling of the experimental data through the fitting of peak positions and shapes. For strong, well-separated peaks, errors in the deconvolution are a few %, while for closely-spaced, weaker peaks (e.g., C1s) the errors may be as large as 10–15%.

3. Results and discussion

3.1. XPS analysis of specimens

Post-irradiation ex situ visual observation of the surface showed no evidence of darkening on the beam spot, confirming the absence of a deposited protective carbon overlayer. This would imply that we were successful in maintaining the C concentration at the surface below 100%, which would correspond to the formation of a protective carbon layer on top of the W surface.

Post-irradiation ex situ XPS analysis of specimens in the present study reveal the presence of C well beyond the ion range; see Fig. 2. In agreement with the visual observations, the XPS depth profiles confirm the absence of a carbon-protecting layer, and therefore, the ion beams were interacting with the mixed surface, containing both W and C – according to our experimental plan. The presence of C at depths greater than 30 nm is explained by the diffusion of C atoms when the surface temperature exceeded 1073 K [19]. The elevated concentrations of C and O within a few nm of the surface are attributed to surface contamination during post-irradiation air exposure.

3.2. Deuterium reemission

The atomic and molecular deuterium reemission results were obtained over several days with overnight interruptions. Following the procedure in Ref. [15], a square root ($T_{specimen}$) correction was applied to the LOS signals to account for the lower ionization probability of faster-moving particles in the QMS ionizer. The data shown in Fig. 3 were taken during several days with 4–6 points taken in a particular day, corresponding to about 60–100% of the temperature range. A run at room temperature was performed each day and the rest of the data were normalized to the RT value for that day. In presenting the data, we have separated the results

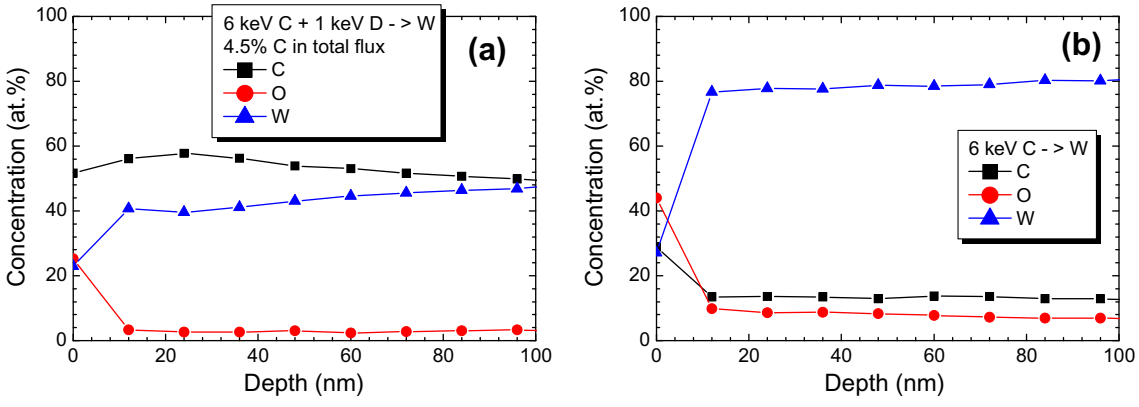

Fig. 2. Post-irradiation XPS depth profiles. (a) Specimen exposed simultaneously to 1 keV D^+ and 6 keV C^+ with total flux of 1.1×10^{19} m^{-2} s^{-1} (4.5% C fraction in total flux); surface temperature was varied in the range 300–1200 K. (b) Specimen exposed to C^+ with flux of 5×10^{17} C^+ m^{-2} s^{-1}; surface temperature was fixed at 1373 K. (Based on the sputter beam parameters, the estimated sputtering rate for these measurements is 0.4 nm/s.).

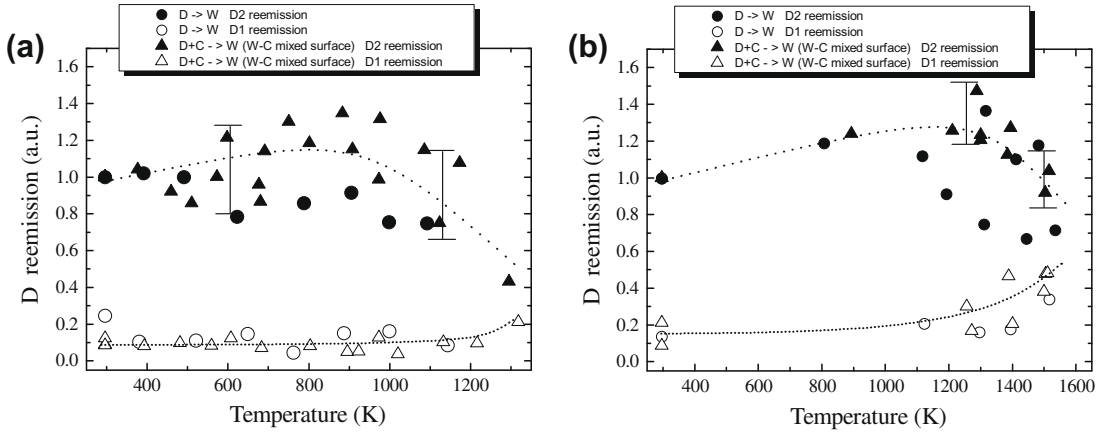

Fig. 3. Reemission of atomic and molecular deuterium from pure W and mixed W–C–D surfaces. Experimental data were acquired during several days. The surface was exposed to a 1 keV D^+ beam (circles) or to simultaneous irradiation with 6 keV C^+ and 1 keV D^+ beams (triangles) with ~4.5% C fraction in the total flux of 1.1×10^{19} m^{-2} s^{-1}. (a) Temperature range: 300–1200 K; (b) Temperature range up to 1200 K. The lines are drawn to guide the eyes.

into two temperature ranges: 300–1200 K in Fig. 3a and 800–1500 K in Fig. 3b. A different specimen was used for each of the two temperature ranges. During a particular experiment, specimens were exposed to both D^+-only and combined C^+ and D^+ irradiations. For both cases, the beams were on continuously and all LOS-QMS measurements were taken with the beams on. Having both beams on all the time during simultaneous C^+–D^+ irradiations provided a stable elemental surface composition.

In the 300–1200 K range any C diffusion into the W substrate is not expected to deplete the carbon from the mixed W–C–D surface layer [19]. In addition, this low-temperature range is characterized by a relatively temperature-independent atomic D reemission from pure W according to both the present results and those in [15]. Indeed, XPS has confirmed the presence of ~50 at.% C to a depth of >100 nm; see XPS profiles in Fig. 2a. Although the D_2 reemission in Fig. 3a shows considerable scatter, the following trends are noted. Reemission from the W–C–D layer exhibits a slight increase over the 300–1000 K range, similar to that found for pure W in [15]. However, the reemission from pure W in the present study appears to be flat within the scatter, perhaps due to insufficient data points. Above 1000 K, the D_2 reemission shows signs of a decreasing trend, although this is largely based on the single point at ~1300 K. While we would expect a corresponding increase in atomic D reemission, the few points above ~1200 K are insufficient to draw any conclusion.

With the second specimen, we have extended the reemission experiment to 1500 K, with emphasis on the 1100–1500 range, where C diffusion becomes more prominent. In this case, we anticipate somewhat lower near-surface C concentrations due to the faster diffusion. Notwithstanding the scatter in the data in Fig. 3b, a noticeable decreasing trend with increasing temperature is observed in the D_2 reemission for temperatures above ~1200 K for both pure W and mixed W–C–D. As expected, the decreasing trend in D_2 reemission is accompanied by an increasing trend in atomic D reemission for both pure and mixed W–C–D.

Comparison of these findings with those of Davis and Haasz [15] leads to the conclusion that the temperature dependence of atomic and molecular deuterium reemission is similar for pure W and mixed W–C–D materials.

3.3. Radiation-enhanced sublimation of carbon

Using a 6 keV C^+ ion beam, C reemission from pure carbon (pyrolytic graphite) and a W–C layer formed during C^+ irradiation of pure tungsten was studied as a function of temperature. The pure carbon experiments were performed to confirm that the experimental setup and procedure will reproduce previous RES results obtained in our laboratory at the University of Toronto [20]. Fig. 4a shows the temperature dependence of C reemission from a pure C surface. Although there is noticeable scatter in the data, one observes a relatively constant C reemission over the temperature range 300–1200 K, confirming previously published findings that RES is negligible at temperatures below 1200 K, e.g., [13,14,20]. For temperatures above approximately 1200 K, the C reemission increases steeply with increasing temperature – a trend characteristic of RES [13,14,20]. We note that some of the LOS-QMS signals were relatively small; the negative signals recorded in Figs. 4a and b might give a minimum estimation of the measurement error.

The RES model, developed by Phillips et al. [21], proposes that interstitial C atoms created by energetic-particle bombardment are able to diffuse to the surface and sublimate with activation energy much less than that for thermal sublimation. This leads to C emission during irradiation of graphite with energetic particles, which increases exponentially with temperature. Therefore, the present experimental C reemission data, normalized by dividing the reemitted C flux by the incident C^+ flux, were fit to the following exponential function:

$$Y = Y_0 \times e^{T/T_0},$$

where T is the surface temperature in K; Y is the C reemission yield C/C^+; $Y_0 = 3.4577 \times 10^{-5}$ C/C^+; $T_0 = 175$ K. Both Y_0 and T_0 were obtained from the present experimental data. The solid line in Fig. 4a shows the exponential fit to the present experimental C reemission data for graphite.

Now we turn to the study of C reemission via RES from a W–C surface during C^+ irradiation at 'high' temperature. Unfortunately, the temperature range for the W–C layer is constrained at both the low and high end. At surface temperatures below about 1073 K, C^+ irradiation would result in the formation of a carbon overlayer. On the other hand, at higher temperatures, carbon diffuses faster into tungsten, potentially leaving a carbon-free surface. Another limitation at the upper end is due to the experimental capability of heating the specimen.

With the limited temperature range, we could not study the temperature dependence of RES from the W–C layer. However, we could study the C^+ fluence dependence of RES (if it were to occur) at a fixed temperature. Since the rate of C depletion from the surface due to diffusion increases with increasing temperature, we have selected 1373 K as the test temperature. This is high enough

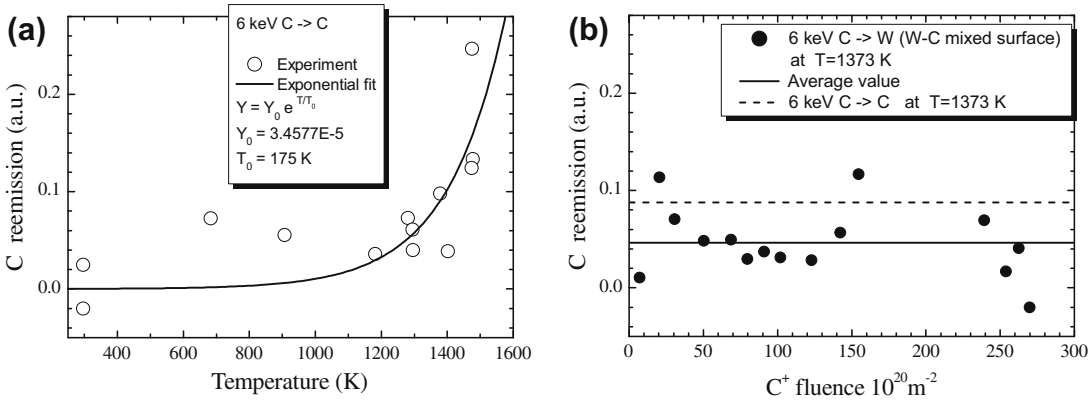

Fig. 4. Intensity of reemitted C due to RES. Both plots have the same scale. Experimental data were acquired during several days. (a) Intensity of temperature dependent RES emission from pure carbon irradiated with 6 keV C^+. The solid line shows the exponential fit to the data. (b) Intensity of reemitted C flux from mixed W–C irradiated with 6 keV C^+ at 1373 K as a function of C^+ fluence. The solid line shows the average value of the RES signal (0.047); the dashed line (~0.088) represents the value obtained from the fit to the pure carbon RES data in Fig. 4a for 1373 K.

to prevent the formation of a carbon overlayer, and high enough to produce RES-type C reemission, but low enough to keep the system (power supplies, residual pressure, specimen integrity) stable for a long time. The desired surface conditions were confirmed by post-irradiation ex situ XPS, which shows 12–15 at.% C concentration at the top surface, with C extending several hundred nm (well beyond the 6 keV C^+ ion range) due to diffusion; see Fig. 2b.

Fig. 4b shows the intensity of the reemitted C flux from the W–C layer, as a function of incident C^+ fluence, plotted on the same scale as Fig. 4a. The data were obtained during 4 days of running with the experiments stopped during nights. In this experiment, steady-state conditions related to surface C coverage were established (i.e., C implantation, sputtering and diffusion were balanced). Within the scatter of the data, we cannot discern any C^+ fluence dependence. The average value of the C reemission (0.047 in arbitrary units) is shown by the solid line in Fig. 4b. On the same plot, the dashed line represents the RES for pure carbon at 1373 K (~0.09 on the same scale as the W–C data) obtained from the experimental fit to the pure carbon RES data in Fig. 4a. Notwithstanding the scatter, the C reemission from the mixed W–C layer is generally lower than the pure carbon value. Unfortunately, since we could not study the temperature dependence of C reemission from the mixed W–C we cannot say whether the generally lower value prevails at temperatures other than 1373 K. The mechanism for RES [21] relies on the transport of C interstitials to a surface where they may desorb. The nature of the mixed C–W surface layer may act to impede this transport, as compared to pure graphite.

It is of particular interest whether RES-type C reemission takes place at temperatures below 1073 K, i.e., where diffusion does not deplete the carbon from the surface. At normal angle of incidence, the absence of diffusion at temperatures below 1073 K leads to the deposition of a carbon overlayer on the W surface. To prevent this from occurring, in one of our experiments we irradiated the surface of a W specimen with 6 keV C^+ ions at an incidence angle of $\alpha = 50°$. It has been shown by Eckstein and Roth [22] that at this incidence angle, C sputtering and deposition are expected to be balanced, providing steady-state conditions (i.e., fluence independent C depth profile) for a mixed W–C surface. The post-irradiation ex situ XPS depth profiles shown in Fig. 5 confirm that no protective carbon layer was formed on the specimens irradiated at both 300 K (RT) and 973 K. We note that the XPS profiles are quite similar: C concentration at the very surface is about 40–50%; it is decreasing deeper into the surface until a depth of ~20 nm. The slight differences can be attributed to surface roughness and contamination during post-irradiation air exposure. We conclude that there is no significant erosion mechanism (RES or otherwise) contributing to the removal of carbon at 973 K as compared to 300 K.

The specimen irradiated at 973 K with 6 keV C^+ at an incidence angle of $\alpha = 50°$ (shown in Fig. 5b) was analyzed by XPS for chemical bonding. The concentrations of atoms (C or W) in a given chemical state are calculated relative to the total number of atoms

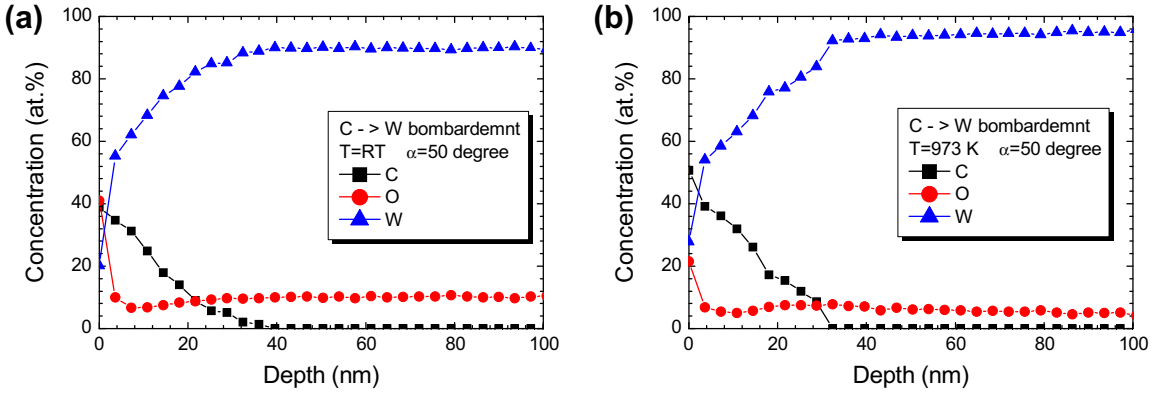

Fig. 5. Post-irradiation XPS depth profiles for W specimens irradiated with 6 keV C^+ ions at 50° incidence angle. Steady-state conditions were achieved for the mixed W–C surface during C^+ irradiations. (a) Specimen irradiated at room temperature; and (b) specimen irradiated at 973 K. (Based on the sputter beam parameters, the estimated sputtering rate for these measurements is 0.12 nm/s.).

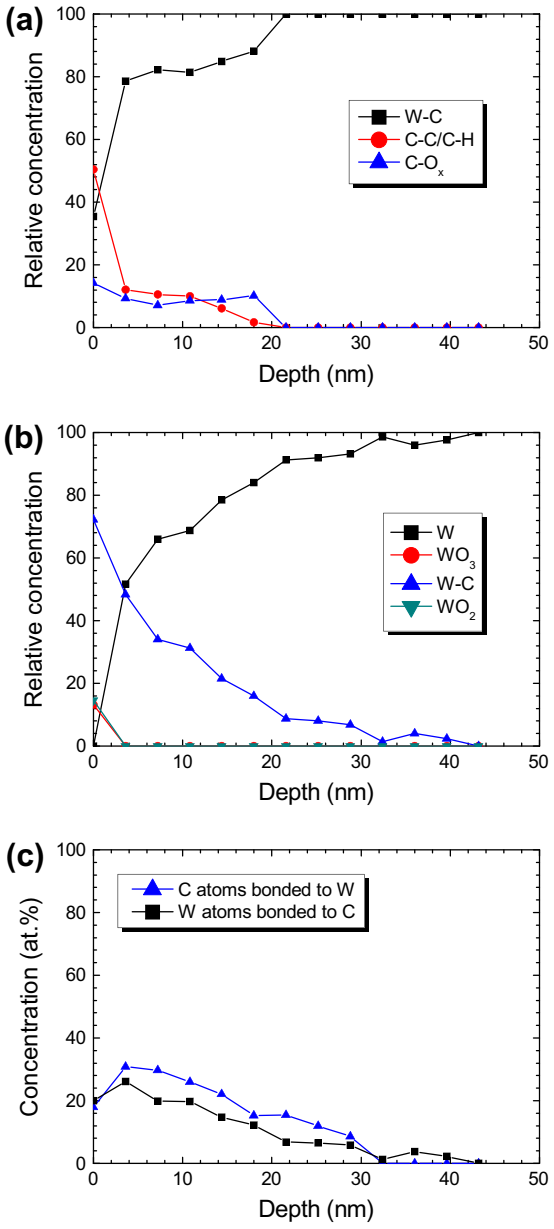

Fig. 6. Post-irradiation XPS depth profiles of the chemical bonding states for W specimens irradiated with 6 keV C^+ ions at 50° incidence angle at 973 K. (This is the same surface, whose elemental depth profiles are shown in Fig. 5b). (a) Relative bond concentrations corresponding to the C1s spectrum; (b) relative bond concentrations corresponding to the W4f spectrum; and (c) the depth profiles of C atoms bonded to W atoms (derived from Figs. 5b and 6a), and of W atoms bonded to C atoms (derived from Figs. 5b and 6b).

at a given depth; see Fig. 6. For example, according to Fig. 6a, 100% of the C atoms beyond 20 nm are bonded to W; however, the total number of C atoms at this depth is very low. One can conclude from Fig. 6a that, apart from the contamination of the top surface, most of the implanted C atoms form carbides with W. The remainder, about 20% of the implanted C, forms either oxides or hydrides.

Fig. 6b shows that in the implantation zone (~20 nm) the decreasing trend of the carbide concentration is similar to the decreasing trend of the implanted C shown in Fig. 5b. Comparing the concentration of carbon atoms bonded to tungsten, derived from Figs. 5b and 6a, with the concentration of tungsten atoms bonded to carbon, derived from Figs. 5b and 6b, one can see that there is, on average, one C atom bonded to W for each W atom bonded with C, see Fig. 6c. It appears that C forms mostly single tungsten carbide, and thus, nearly all implanted C atoms are retained primarily in the form of WC.

4. Conclusions

We have measured the reemission of D and C from mixed W–C and W–C–D layers using line-of-sight quadrupole mass spectroscopy during irradiation of W specimens with either C^+ only or with combined D^+ and C^+. The results for simultaneous D^+–C^+ irradiations show that the temperature dependence of the reemitted flux of atomic and molecular deuterium from a mixed W–C–D surface is generally similar to those of pure W. A noticeable decreasing trend with increasing temperature is observed in the D_2 reemission for temperatures above ~1200 K for both pure W and mixed W–C–D. As expected, the decreasing trend in D_2 reemission is accompanied by an increasing trend in atomic D reemission for both pure and mixed W–C–D.

Carbon reemission from a mixed W–C layer measured at 1373 K over an extended fluence range was found to be lower than C reemission from pure carbon; the RES value for W–C is about half the value for pure C at 1373 K.

Post-irradiation XPS analysis of the chemical bonding states of a W specimen irradiated at 973 K with 6 keV C^+ shows that carbon in the mixed W–C surface is primarily in the form of WC.

Acknowledgements

We gratefully acknowledge the funding from the Natural Sciences and Engineering Research Council of Canada. We thank Charles Perez for his continual technical assistance in ensuring the smooth operation of the experimental facility.

References

[1] G. Janeschitz, et al., J. Nucl. Mater. 290–293 (2001) 1.
[2] D. Meade, S.C. Jardin, J.A. Schmidt, et al., Mission and design of the fusion ignition research experiment, in: Proceedings of the 18th IAEA Conference on Fusion Energy, Sorrento, Italy, October, 2000, (CD-ROM), pp. IAEA-CN-77/FTP2/16, IAEA, Vienna, 2001.
[3] S. Nishio, K. Ushigusa, S. Ueada, et al., Conceptional design of advanced steady-state tokamak reactor, in: Proceedings of the 18th Conference on Fusion Energy, Sorrento, Italy, October, 2000, (CDROM), pp. IAEA-CN-77/FTP2/14, IAEA, Vienna, 2001.
[4] A.S. Kukushkin, H.D. Pacher, D.P. Coster, et al., J. Nucl. Mater. 337–339 (2005) 50.
[5] K. Schmid, K. Krieger, A. Kukushkin, A. Loarte, J. Nucl. Mater. 363–365 (2007) 674.
[6] K. Schmid, J. Roth, J. Nucl. Mater. 313–316 (2003) 302.
[7] I. Bizyukov, K. Krieger, J. Appl. Phys. 101 (2007) 104906.
[8] I. Bizyukov, K. Krieger, J. Appl. Phys. 102 (2007) 074923.
[9] I.A. Bizyukov, J.W. Davis, A.A. Haasz, P. Brodersen, J. Nucl. Mater. 390–391 (2009) 925.
[10] H.T. Lee, K. Krieger, J. Nucl. Mater. 390–391 (2009) 971.
[11] Y. Oya, Y. Inagaki, S. Suzuki, et al., J. Nucl. Mater. 390–391 (2009) 622.
[12] A.A. Haasz, J.W. Davis, J. Nucl. Mater. 175 (1990) 84.
[13] J. Roth, J. Bohdansky, K.L. Wilson, J. Nucl. Mater. 111–112 (1982) 775.
[14] V. Philipps, K. Flaskamp, E. Vietzke, J. Nucl. Mater. 111–112 (1982) 781.
[15] J.W. Davis, A.A. Haasz, J. Nucl. Mater. 223 (1995) 312.
[16] J.W. Davis, A.A. Haasz, Nucl. Instrum. Meth. B83 (1993) 117.
[17] W. Eckstein, Calculated Sputtering, Reflection and Range Values, IPP Report 9/132, 2002.
[18] W. Moeller, W. Eckstein, J.P. Biersack, Comput. Phys. Commun. 51 (1988) 355.
[19] K. Schmid, J. Roth, W. Eckstein, J. Nucl. Mater. 290–293 (2001) 148.
[20] P. Franzen, J.W. Davis, A.A. Haasz, J. Appl. Phys. 78 (1995) 817.
[21] V. Philipps, E. Vietzke, R.P. Schorn, H. Trinkaus, J. Nucl. Mater. 155–157 (1988) 319.
[22] W. Eckstein, J. Roth, Nucl. Instrum. Meth. B53 (1991) 279.